

US EPA ARCHIVE DOCUMENT



Numerical Modeling of Selected Sediment Traps in Kalamazoo River, Michigan

Zhenduo Zhu¹
Marcelo H. Garcia²

¹Graduate Research Assistant

²Professor and Director

Ven Te Chow Hydrosystems Laboratory

Prepared for:

U.S. Environmental Protection Agency

Region 5

Chicago, IL 60604-3590



Ven Te Chow Hydrosystems Laboratory

Civil and Environmental Engineering

University of Illinois

Urbana, Illinois

June 2015

**Numerical Modeling of Selected Sediment Traps in
Kalamazoo River, Michigan**

by

Zhenduo Zhu and Marcelo H. García

Ven Te Chow Hydrosystems Laboratory
Department of Civil and Environmental Engineering
University of Illinois at Urbana and Champaign, IL



Table of Contents

Executive Summary	6
1. Introduction.....	7
2. Description of the Numerical Models.....	8
2.1 Computational Meshes.....	8
2.2 Bathymetry.....	10
2.3 Model Scenarios and Boundary Conditions	12
3. Results of MP 10.4&10.5 Sediment Trap Model.....	17
3.1 Distribution of Depth-Averaged Velocity Magnitude.....	17
3.2 Distribution of Bed Shear Stress.....	21
4. Results of MP 14.75 Sediment Trap Model.....	23
4.1 Distribution of Depth-Averaged Velocity Magnitude.....	23
4.2 Distribution of Bed Shear Stress.....	26
4.3 An Example Run of Sediment Transport Simulation (100-year Flood Scenario) .	28
5. Results of MP 21.5 Sediment Trap Model.....	31
5.1 Distribution of Depth-Averaged Velocity Magnitude.....	31
5.2 Distribution of Bed Shear Stress.....	33
6. Summary.....	36
Acknowledgments.....	37
Bibliography	38

Table of Figures

Figure 1. Location of Modeled Sediment Traps	7
Figure 2. Computational Meshes of MP 10.4&10.5 Sediment Trap	9
Figure 3. Computational Meshes of MP 14.75 Sediment Trap	9
Figure 4. Computational Meshes of MP 21.5 Sediment Trap	10
Figure 5. Bed Elevation of River and Floodplain at MP 10.4&10.5 Sediment Trap.....	11
Figure 6. Bed Elevation of River and Floodplain at MP 14.75 Sediment Trap.....	11
Figure 7. Bed Elevation of River and Floodplain at MP 21.5 Sediment Trap.....	12
Figure 8. Flow Statistics for the Kalamazoo River at Comstock, MI (based on 1933-2013 data)	13
Figure 9. Boundary Conditions of April 9-29, 2013 at MP 10.4&10.5 Sediment Trap.....	13
Figure 10. Boundary Conditions of July 11-19, 2013 at MP 10.4&10.5 Sediment Trap	14
Figure 11. Boundary Conditions of April 9-29, 2013 at MP 14.75 Sediment Trap.....	14
Figure 12. Boundary Conditions of July 11-19, 2013 at MP 14.75 Sediment Trap	15
Figure 13. Boundary Conditions of April 9-29, 2013 at MP 21.5 Sediment Trap.....	15
Figure 14. Boundary Conditions of July 11-19, 2013 at MP 21.5 Sediment Trap	16
Figure 15. Distribution of Velocity Magnitude (MP10.4&10.5, 20:00 April 13, 2013).....	18
Figure 16. Distribution of Velocity Magnitude (MP10.4&10.5, 8:00 April 21, 2013).....	18
Figure 17. Distribution of Velocity Magnitude (MP10.4&10.5, 20:00 July 17, 2013)	19
Figure 18. Flow Path and Recirculation Zones (MP10.4&10.5, 8:00 April 21, 2013).....	19
Figure 19. Survey of Submerged Oil in the Modeling Domain of MP 10.4&10.5 (figure from the Enbridge Energy, L.P. report [1])	20
Figure 20. Distribution of Bed Shear Stress (MP10.4&10.5, 20:00 April 13, 2013)	21
Figure 21. Distribution of Bed Shear Stress (MP10.4&10.5, 8:00 April 21, 2013)	22
Figure 22. Distribution of Bed Shear Stress (MP10.4&10.5, 20:00 July 17, 2013).....	22
Figure 23. Distribution of Velocity Magnitude (MP14.75, 4:00 April 14, 2013).....	23
Figure 24. Distribution of Velocity Magnitude (MP14.75, 12:00 April 21, 2013).....	24
Figure 25. Flow Path at 2 nd Bifurcation and Confluence (MP14.75, 0:00 April 20, 2013)	24
Figure 26. Flow Path at 1 st Bifurcation and Confluence (MP14.75, 0:00 April 20, 2013).....	25
Figure 27. Distribution of Velocity Magnitude (MP14.75, 0:00 July 12, 2013)	25
Figure 28. Distribution of Bed Shear Stress (MP14.75, 4:00 April 14, 2013)	27
Figure 29. Distribution of Bed Shear Stress (MP14.75, 12:00 April 21, 2013)	27
Figure 30. Distribution of Bed Shear Stress (MP14.75, 0:00 July 12, 2013).....	28
Figure 31. Distribution of Velocity Magnitude in 100-year Flood Scenario (MP14.75).....	29
Figure 32. Distribution of Bed Shear Stress in 100-year Flood Scenario (MP14.75)	30
Figure 33. Distribution of Suspended Sediment Concentration in 100-year Flood Scenario (MP14.75).....	30

Figure 34. Distribution of Velocity Magnitude (MP21.5, 16:00 April 14, 2013).....	31
Figure 35. Distribution of Velocity Magnitude (MP21.5, 16:00 April 21, 2013).....	32
Figure 36. Distribution of Velocity Magnitude (MP21.5, 8:00 July 16, 2013)	32
Figure 37. Distribution of Bed Shear Stress (MP21.5, 16:00 April 14, 2013)	33
Figure 38. Distribution of Bed Shear Stress (MP21.5, 16:00 April 21, 2013)	34
Figure 39. Distribution of Bed Shear Stress (MP21.5, 8:00 July 16, 2013).....	34
Figure 40. Survey of Submerged Oil in the Modeling Domain of MP 21.5 (figure from the Enbridge Energy, L.P. report [1])	35

Executive Summary

The July 2010 spill of diluted bitumen into the Kalamazoo River was the largest release of heavy crude into an inland waterway in U.S. history. Since the spill, extensive cleanup and recovery efforts have taken place. However, substantial residual deposits from the oil spill remained in the river system due to formation of oil-particle aggregates (OPA) and their negative buoyancy. It is important to understand the conditions under which the OPA could be entrained into suspension, transported and re-deposited. An in-house numerical code, HydroSed2D, was utilized to simulate OPA transport and settling in selected natural sediment traps (hereafter referred to as sediment traps) along the Kalamazoo River. The sediment traps were constructed to concentrate and hold submerged oil in an attempt to prevent it from migrating downstream before it could be recovered. HydroSed2D program enabled a nested approach with an unstructured mesh design which provided a higher spatial resolution and afforded a more detailed morphology of the sediment traps than could be achieved through the 2-D Environmental Fluid Dynamics Code (EFDC) hydrodynamic and sediment transport models. The HydroSed2D model complemented the 2-D EFDC models which covered a much larger numerical domain but had a coarser computational mesh.

Three sediment traps, MP10.4&10.5, MP14.75, and MP21.5, were chosen to be modeled. Each channel reach had different geomorphic characteristics. It was found that deposition happened under relatively high flow conditions, when river water would flow into the sediment traps and OPAs would deposit due to a reduction in sediment transport capacity associated with low flow velocities and bed shear stresses that were illustrated by the model. The depositional areas indicated by the models agreed in general with the mapped areas where heavy submerged oil was found during field assessments. The models developed during this effort are useful tools in the ongoing cleanup work and may also be useful for future management efforts associated with oil spill accidents.

1. Introduction

Following the oil spill at Kalamazoo River waterways system in 2010, extensive oil cleanup and environmental remediation efforts have taken place. Sediment traps, e.g. cutoff channel and meanders, are very critical areas for the cleanup work and future management because high concentrations of oil-particle aggregates (OPA) have a tendency to deposit there. This facilitates recovery efforts to remove OPAs from the river.

Among many sediment traps in the waterways, three sediment traps were selected for modeling, namely MP10.4&10.5, MP14.75, and MP21.5, because of their importance and representativeness. Figure 1 shows the geomorphic features of the sediment traps. MP10.5 has a backwater channel; MP14.75 has both bifurcation and confluence channels; and MP21.5 is an oxbow.

Three numerical models covering the three river sections (numerical domains) were built. The models facilitated our understanding of the physics of OPA transport and fate in response to flow fields in different kinds of channels. The April 2013 high flow and July 2013 low flow scenarios were simulated. By comparing our models to submerged oil survey data, good agreement was revealed with respect to areas containing heavy submerged oil. The models could be useful tools for management and other purposes.

SELECTED SEDIMENT TRAPS

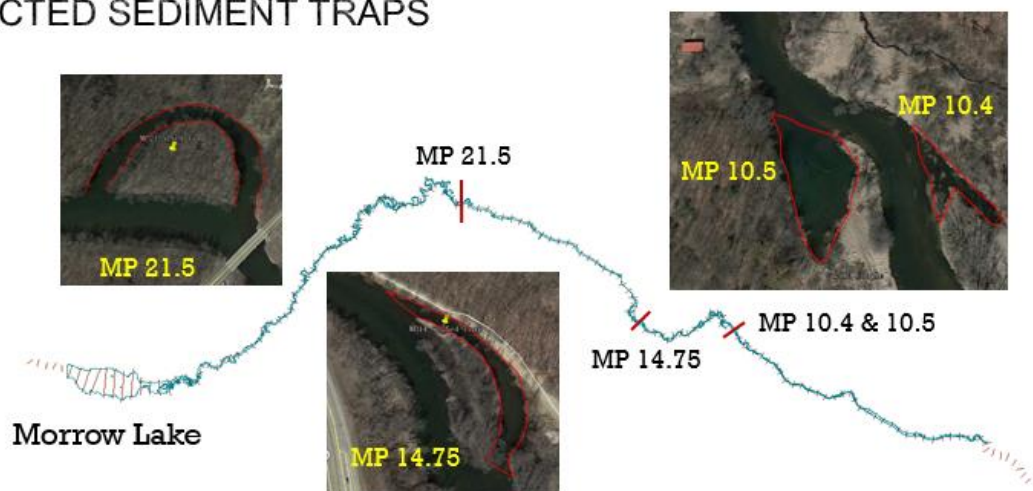


Figure 1. Location of Modeled Sediment Traps along the Kalamazoo River, Michigan

2. Description of the Numerical Models

An in-house code developed at Ven Te Chow Hydrosystems Laboratory, HydroSed2D, was used in this study. HydroSed2D was developed as a two-dimensional shallow water model coupled with a bedload sediment transport model (Liu et al. 2008). Zhu (2011) implemented suspended sediment transport into HydroSed2D. The model has been tested and applied to many studies and has also helped to understand sediment transport problems in floodplains and flood control channels (Zhu et al. 2011, Liu et al. 2012, and Goodwell et al. 2014). The detailed governing equations of HydroSed2D can be found in Zhu (2011). In this study, the scope of the HydroSed2D/sediment trap modeling was limited to the use of the model to simulate hydrodynamic conditions only for two of the sediment trap areas (e.g., MP10.5 and MP21.5), while the hydrodynamic and sediment transport simulations were performed for the third area (MP14.75). Manning's coefficient $n = 0.03$ was used as a constant for all three sediment traps.

2.1 Computational Meshes

The model used finite volume method and unstructured meshes. Unlike structured meshes, unstructured triangular meshes allow modelers to deal with complex geometries. The computational meshes of the three sediment traps are shown in figures 2 to 4. A high degree of spatial resolution was obtained thanks to the use of unstructured meshes which can adapt to complex morphologies.

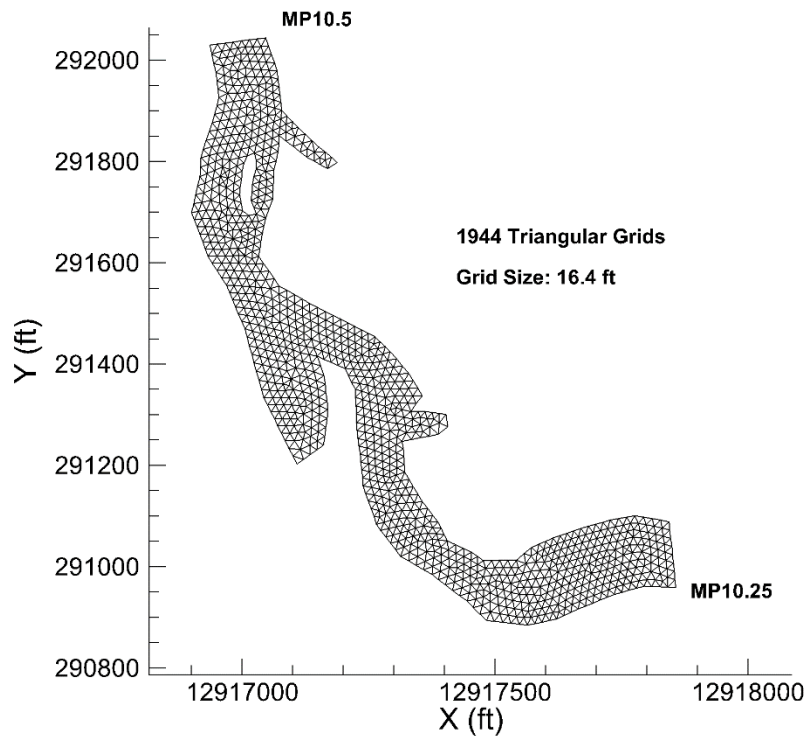


Figure 2. Computational Meshes for MP 10.4&10.5 Sediment Trap

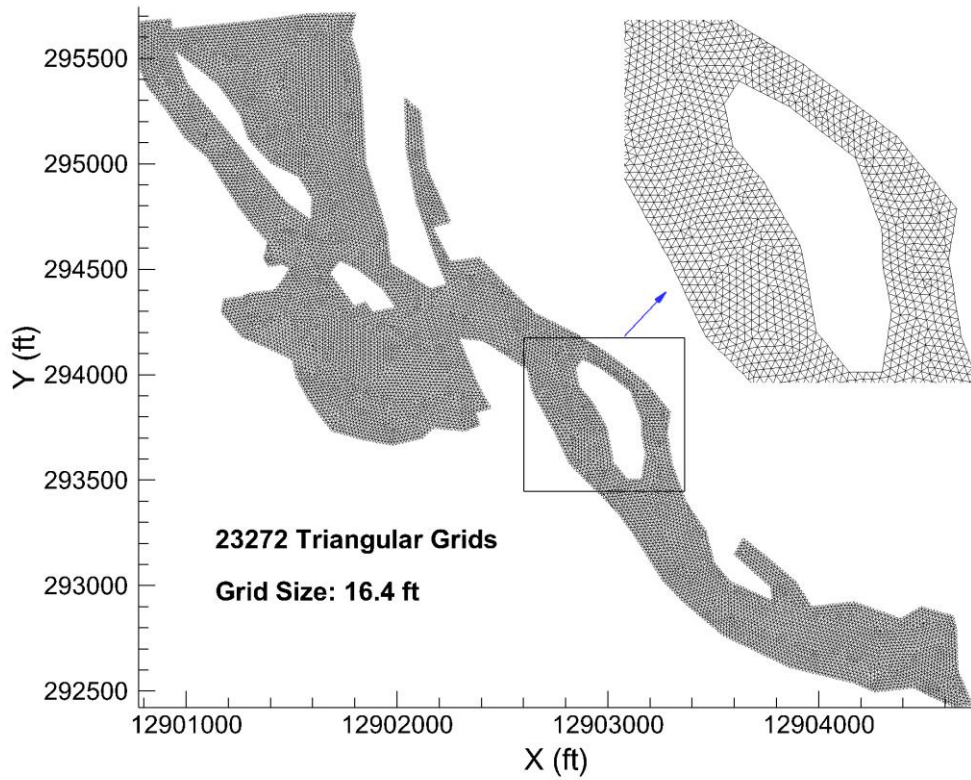


Figure 3. Computational Meshes for MP 14.75 Sediment Trap

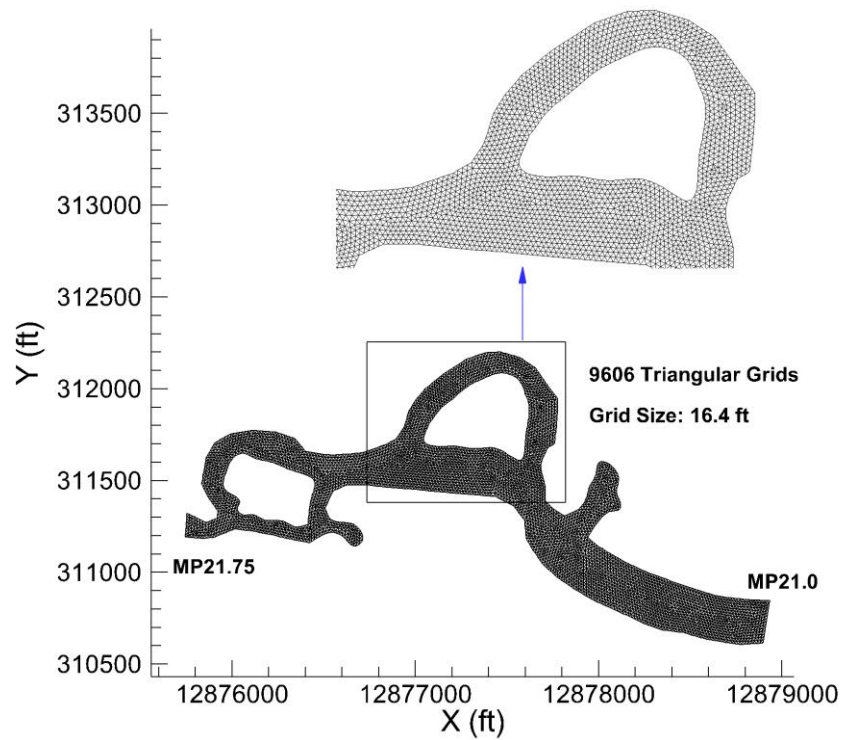


Figure 4. Computational Meshes for MP 21.5 Sediment Trap

2.2 Bathymetry

The bathymetry data of the three sediment traps was provided by Weston Solutions, Inc. (Weston, 2014). River bed elevation was interpolated to the center of each grid. The domain of the MP 14.75 sediment trap included the 100-year floodplain.

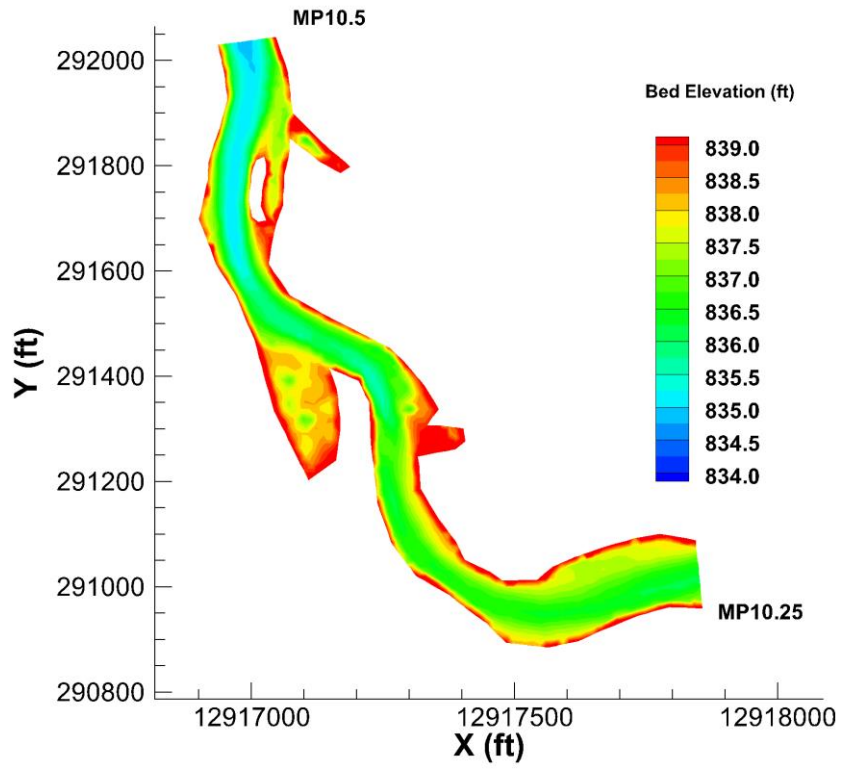


Figure 5. Bed Elevation of River and Floodplain at MP 10.4&10.5 Sediment Trap

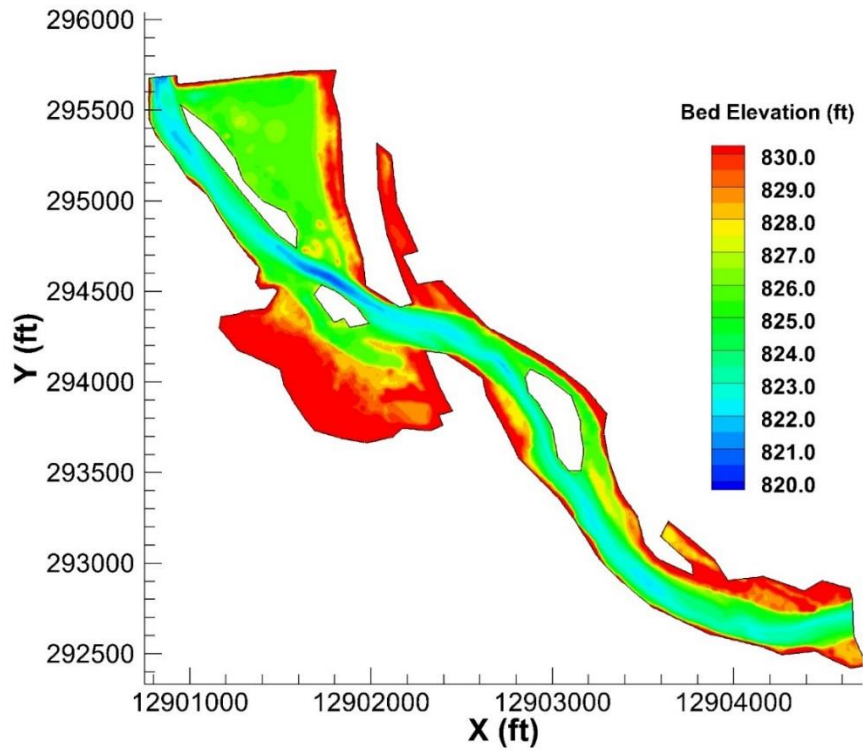


Figure 6. Bed Elevation of River and Floodplain at MP 14.75 Sediment Trap

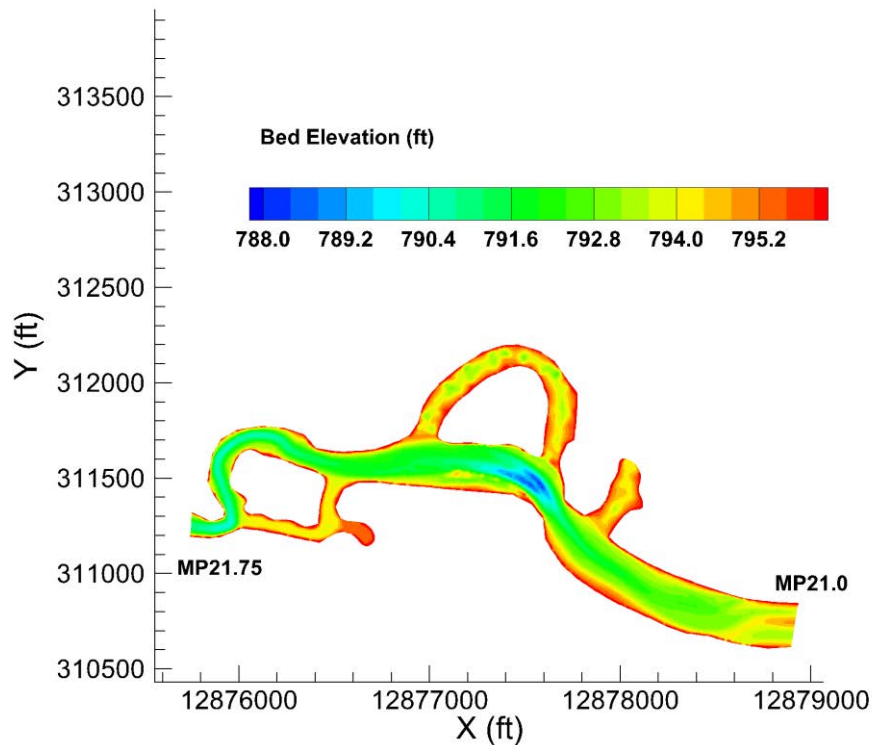


Figure 7. Bed Elevation of River and Floodplain at MP 21.5 Sediment Trap

2.3 Model Scenarios and Boundary Conditions

April 2013 and July 2013 were simulated as representative scenarios of high flow and low flow, respectively. Figure 8 shows the historical flow record (1933-2013) at a USGS gauging station located downstream of Morrow Lake. It indicates that the peak of the April 2013 flow is higher than the 95th percentile of daily mean value for those dates in the last 80 years and the July 2013 flow is slightly under the median daily mean value in July, which is the period corresponding to the lowest flow discharge within a year. The April 2013 high flow has a flood exceedance probability of 4% (25-yr recurrence interval).

For each sediment-trap simulation, upstream flow discharge and downstream water stage level were extracted from the LimnoTech-EFDC2D model (LimnoTech, 2014) and used as boundary conditions. They are shown in Figure 9 to Figure 14.

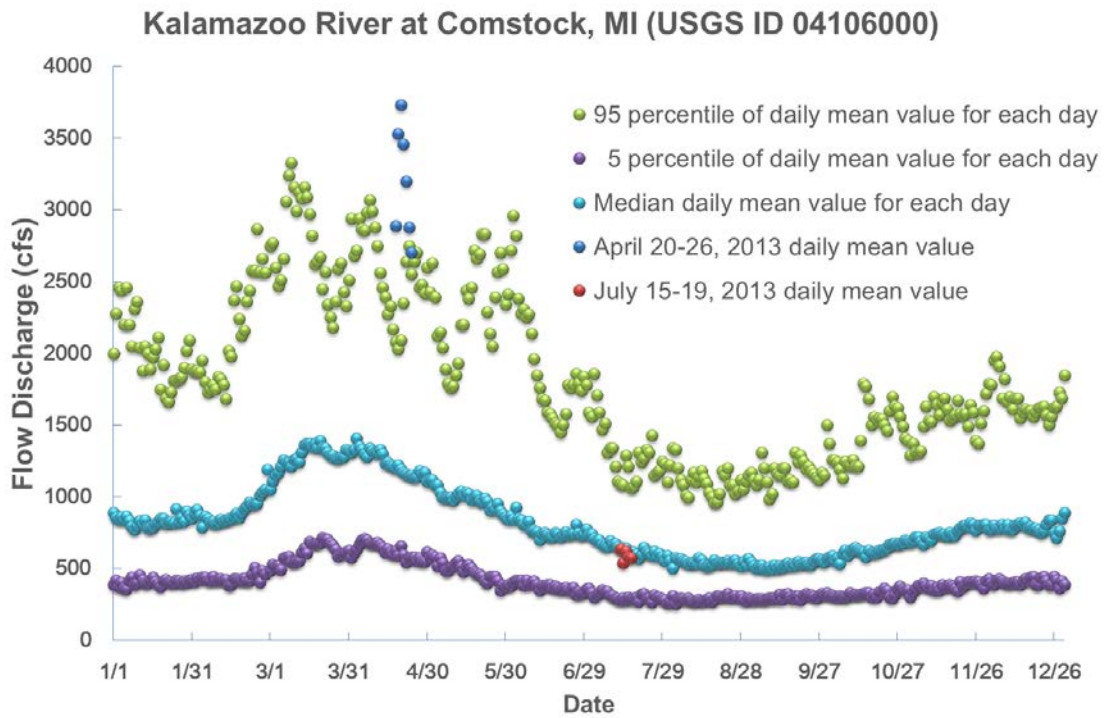


Figure 8. Flow Statistics for the Kalamazoo River at Comstock, MI (based on 1933-2013 data)

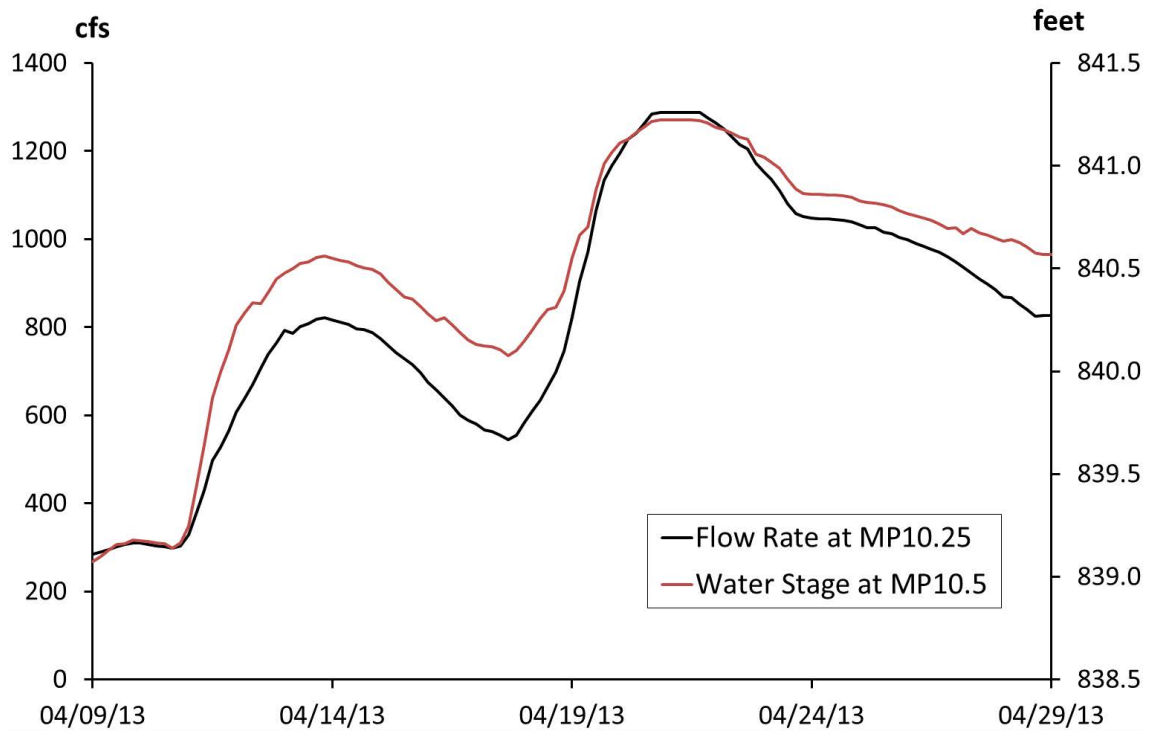


Figure 9. Boundary Conditions for April 9-29, 2013 at MP 10.4&10.5 Sediment Trap

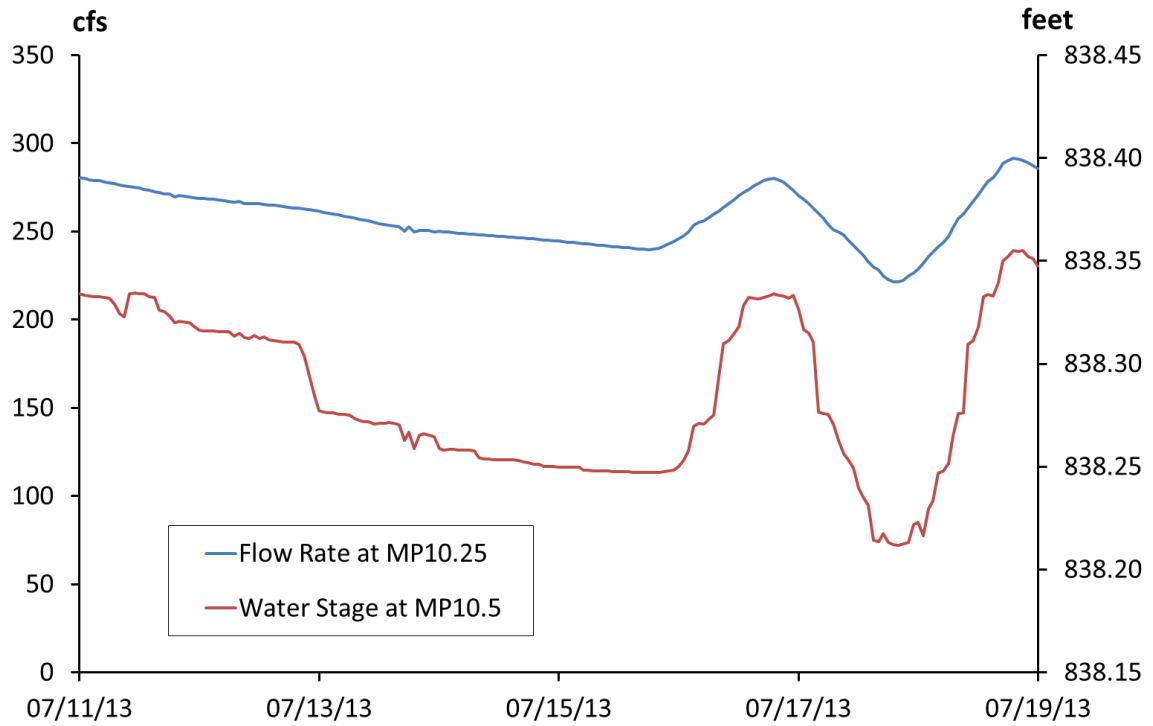


Figure 10. Boundary Conditions for July 11-19, 2013 at MP 10.4&10.5 Sediment Trap

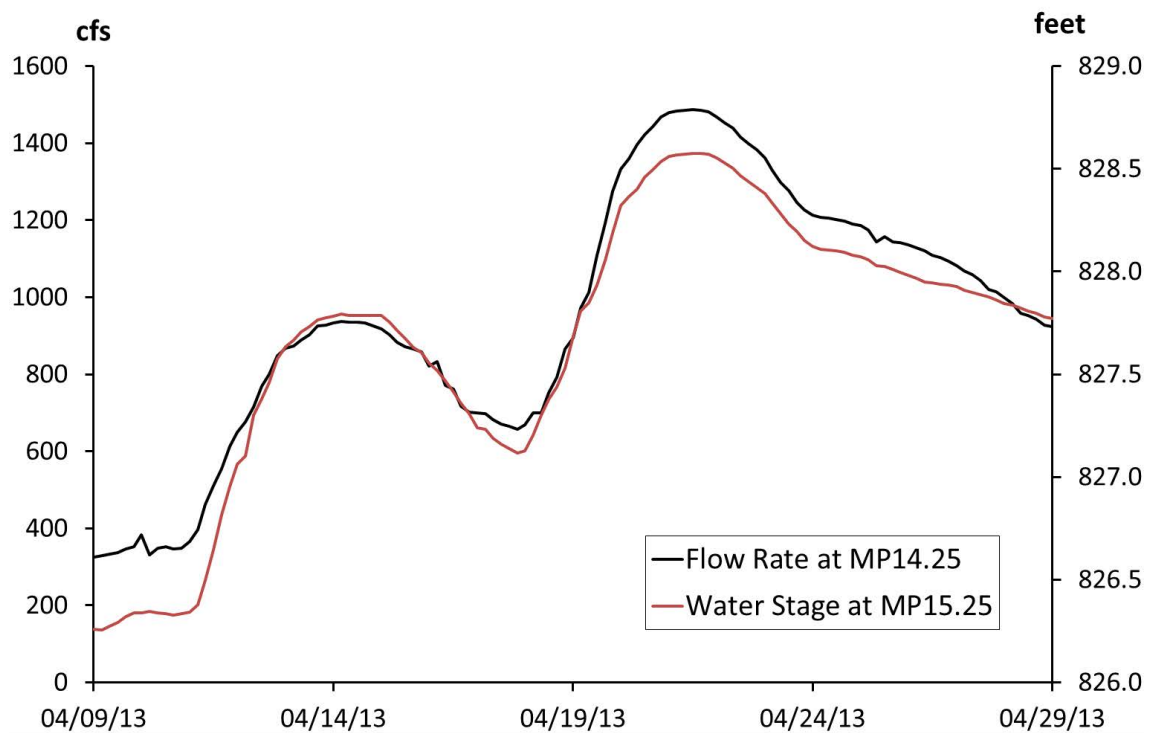


Figure 11. Boundary Conditions for April 9-29, 2013 at MP 14.75 Sediment Trap

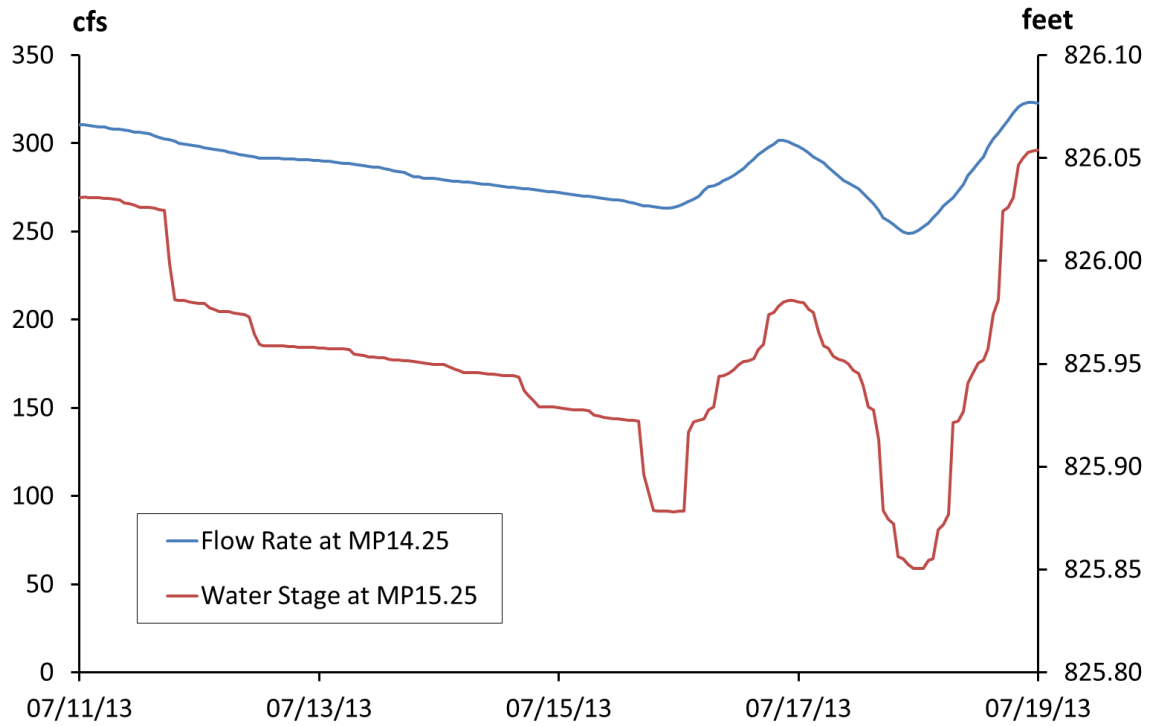


Figure 12. Boundary Conditions for July 11-19, 2013 at MP 14.75 Sediment Trap

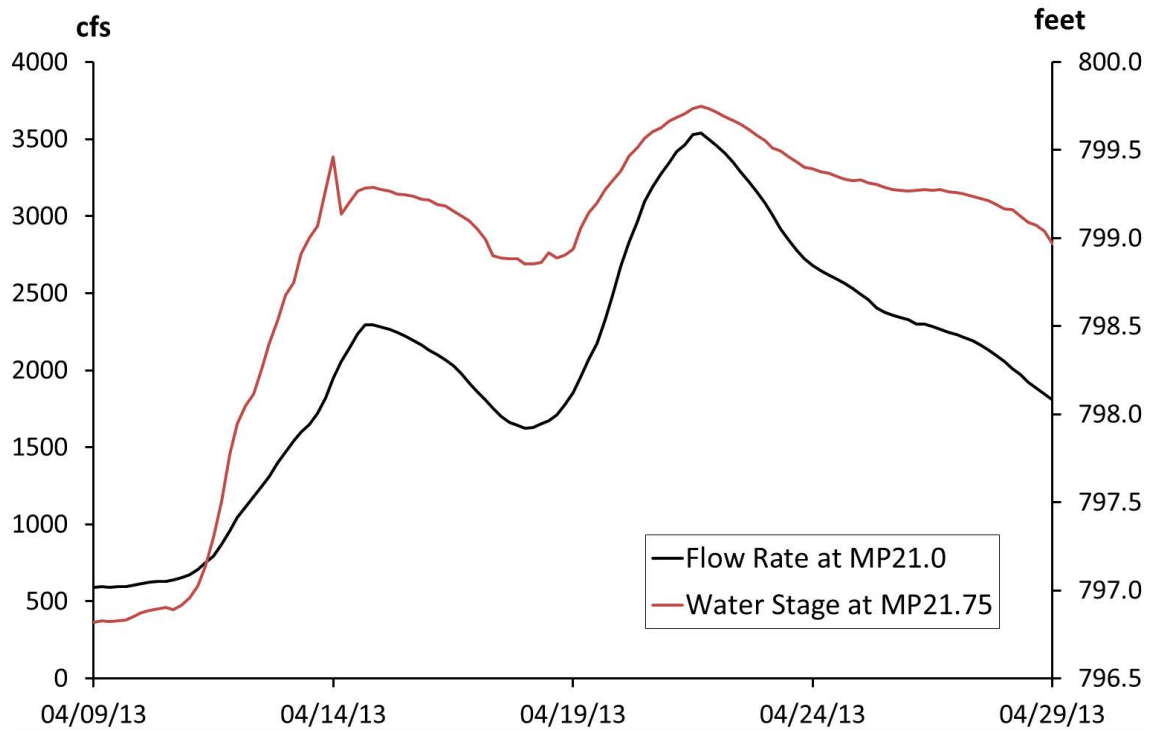


Figure 13. Boundary Conditions for April 9-29, 2013 at MP 21.5 Sediment Trap

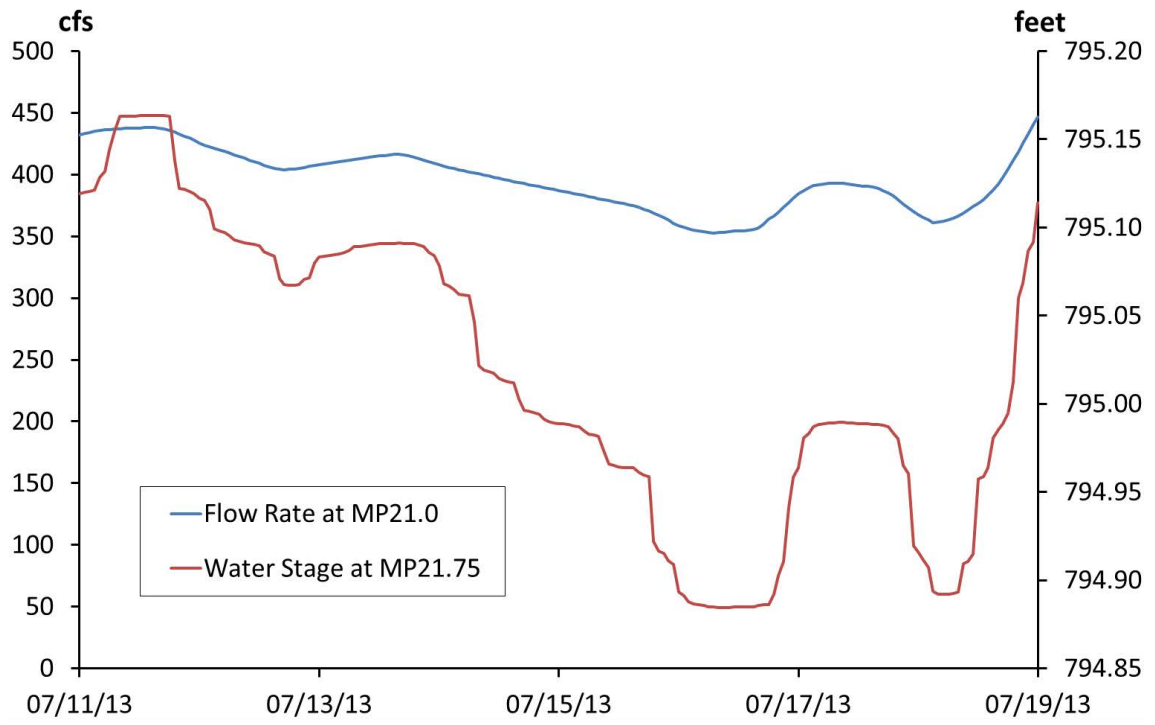


Figure 14. Boundary Conditions for July 11-19, 2013 at MP 21.5 Sediment Trap

3. Results of MP 10.4&10.5 Sediment Trap Model

3.1 Distribution of Depth-Averaged Velocity Magnitude

Figure 15, Figure 16, and Figure 17 show examples of the depth-averaged velocity magnitude in high flow (April 2013) and low flow (July 2013) scenarios. There were two peaks in the April 2013 scenario (see Figure 9) and both of them are plotted. The dry water depth was defined as 0.1 meter, i.e. 0.33 ft. Under the high flow conditions, it is shown that the low velocities are present in the sediment traps MP10.4 and MP10.5. Also, there is a bifurcation channel along the right descending bank north of the sediment traps where velocities are low. However, under the low flow condition, water is constrained in the main channel. The absence of model results shown in the Figure 17 indicates that the simulated water depths were below the minimum model threshold of 10 cm or 0.3 ft. While water below this minimum depth may be present, significant new contributions of water or sediment to the sediment traps are unlikely under these very low flow conditions. The simulations showed that flows and therefore OPAs can enter the trap areas during high flow period and remain there because of the low flow velocities and bed shear stresses. This suggests that the sediment trap is performing well.

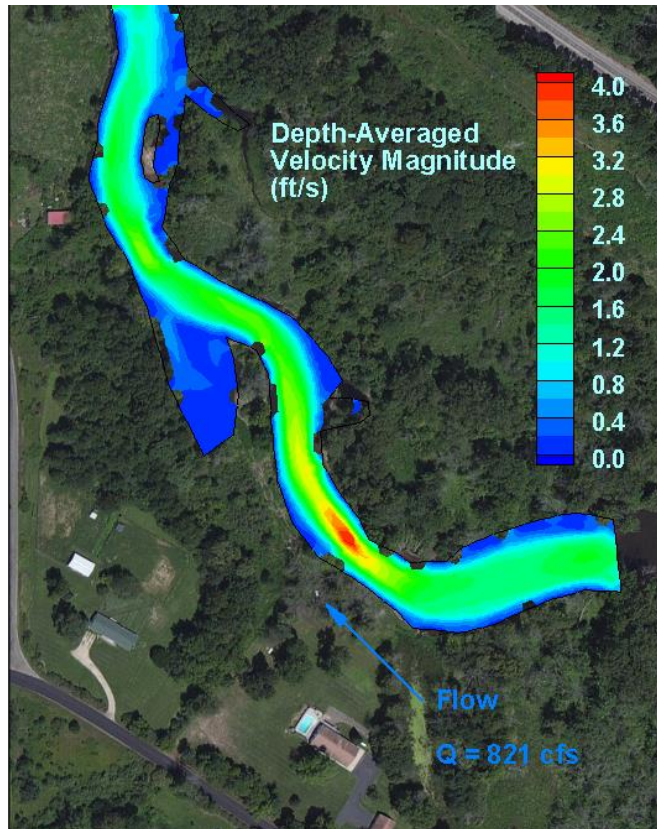


Figure 15. Distribution of Velocity Magnitude (MP10.4&10.5, 20:00 April 13, 2013)

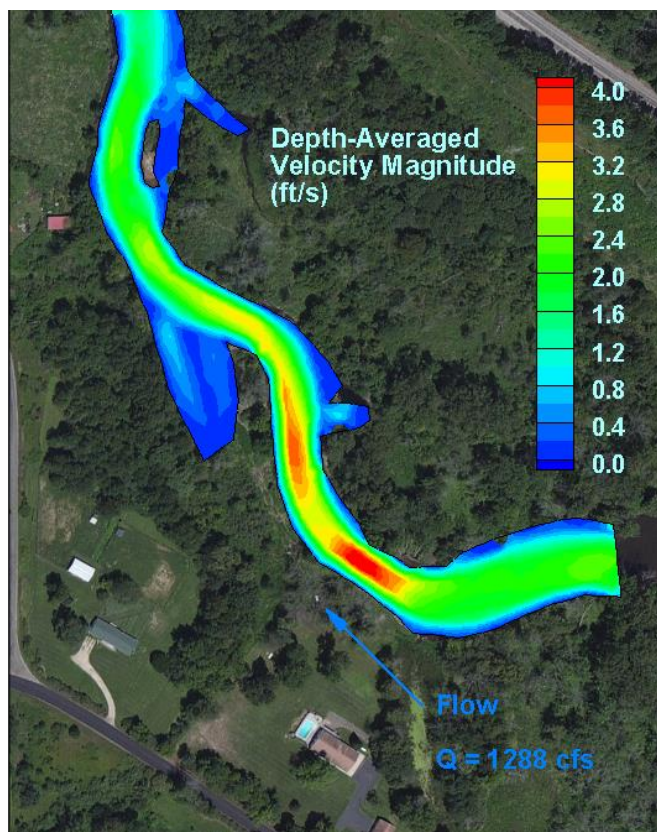


Figure 16. Distribution of Velocity Magnitude (MP10.4&10.5, 8:00 April 21, 2013)

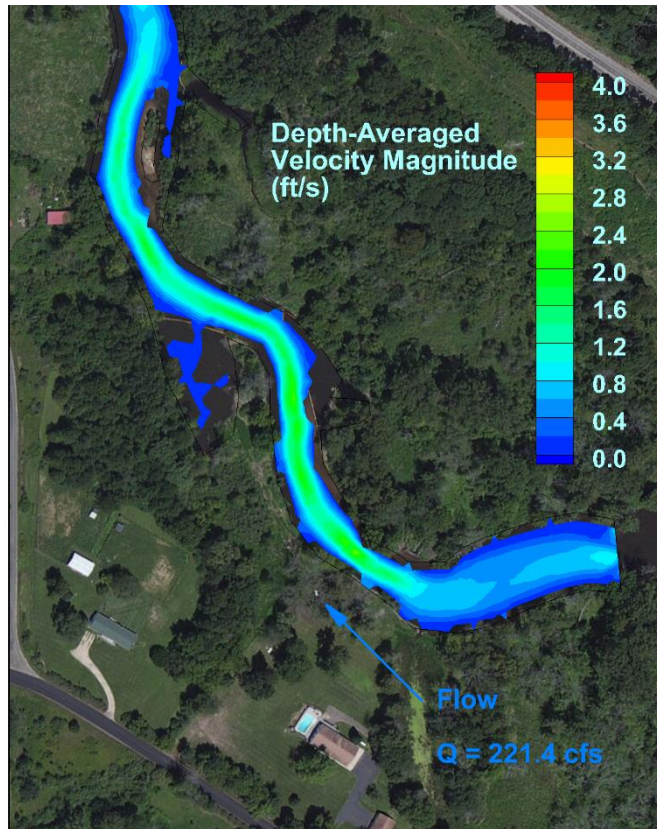


Figure 17. Distribution of Velocity Magnitude (MP10.4&10.5, 20:00 July 17, 2013)

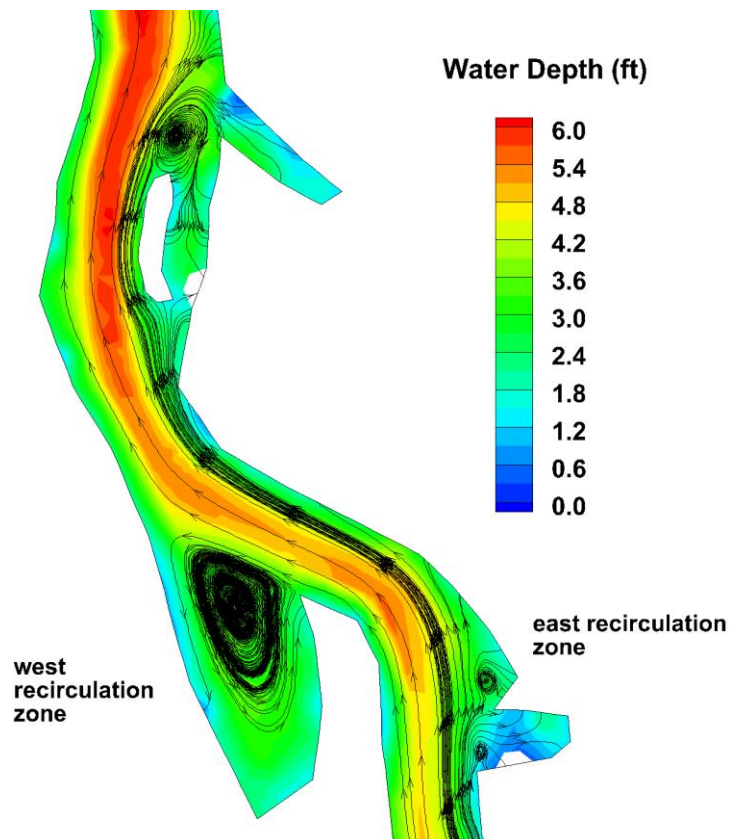


Figure 18. Flow Path and Recirculation Zones (MP10.4&10.5, 8:00 April 21, 2013)

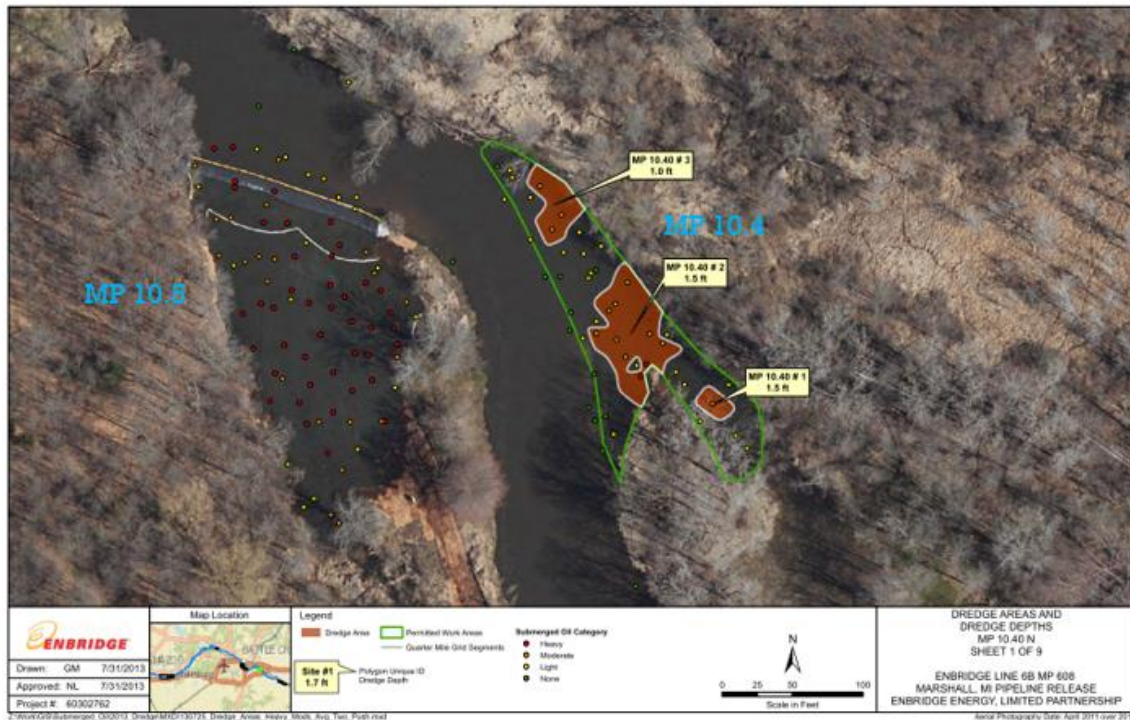


Figure 19. Survey of Submerged Oil in the Modeling Domain of MP 10.4&10.5 (figure from the Enbridge Energy, L.P. report [1])

The deposition areas according to field poling results in this domain are shown in Figure 19. The poling results show a qualitative description of oiled sediment as heavy (red), moderate (orange), light (yellow), and none (blue) in the sediment traps modeled at MP 10.5 site. The reason for deposition is flow recirculation and the loss of sediment transport capacity. The OPAs enter recirculation zones where flow velocities are so small that the flow cannot keep OPAs in suspension. Moreover, recirculation of flow does not allow OPAs to move out of those zones so eventually they end up depositing. Figure 18 shows the flow path of the numerical simulation.

Once the OPAs are entrained into the recirculation zone, the majority are expected to deposit before being re-entrained into the main channel. The west recirculation zone (see Figure 18) could be easily recognized. The east recirculation zone also has the potential to be net depositional. It is also noted that there is another recirculation zone downstream which indicates possible deposition of OPAs.

3.2 Distribution of Bed Shear Stress

Figure 20, Figure 21, and Figure 22 show distributions of bed shear stress for both high and low flow scenarios, respectively. Similar to the velocity magnitude shown above, the bed shear stress in the main channel is higher than that in the sediment traps and an east side channel further downstream during high flow events.

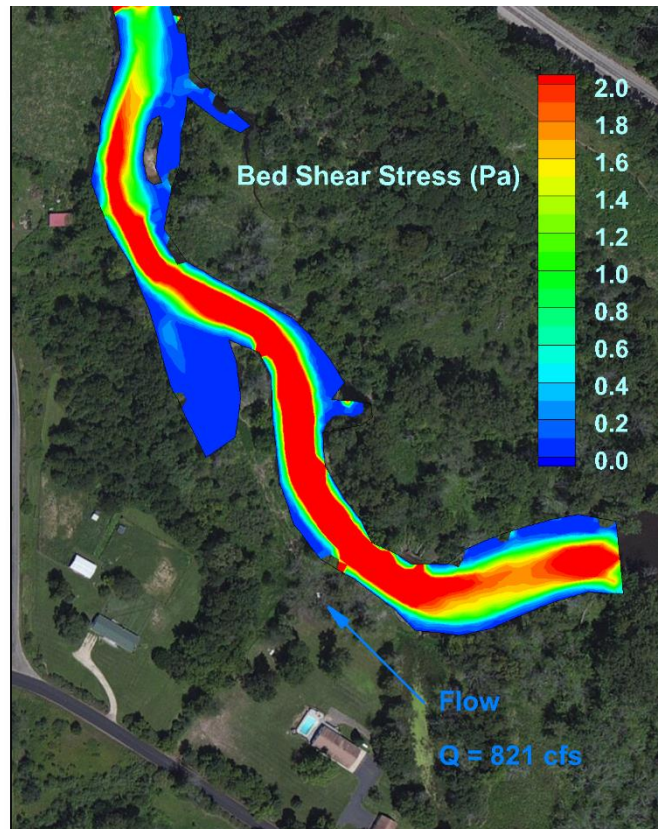


Figure 20. Distribution of Bed Shear Stresses (MP10.4&10.5, 20:00 April 13, 2013)

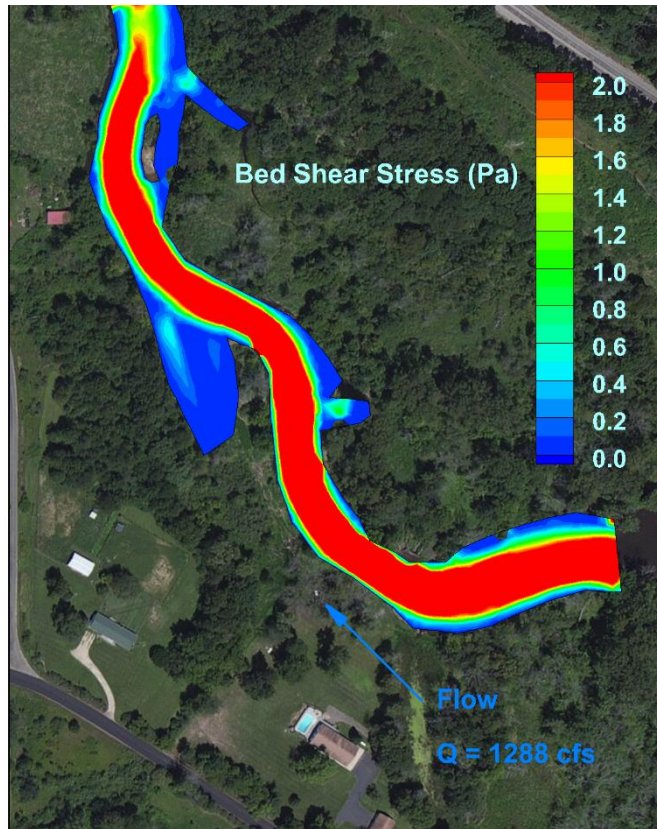


Figure 21. Distribution of Bed Shear Stresses (MP10.4&10.5, 8:00 April 21, 2013)

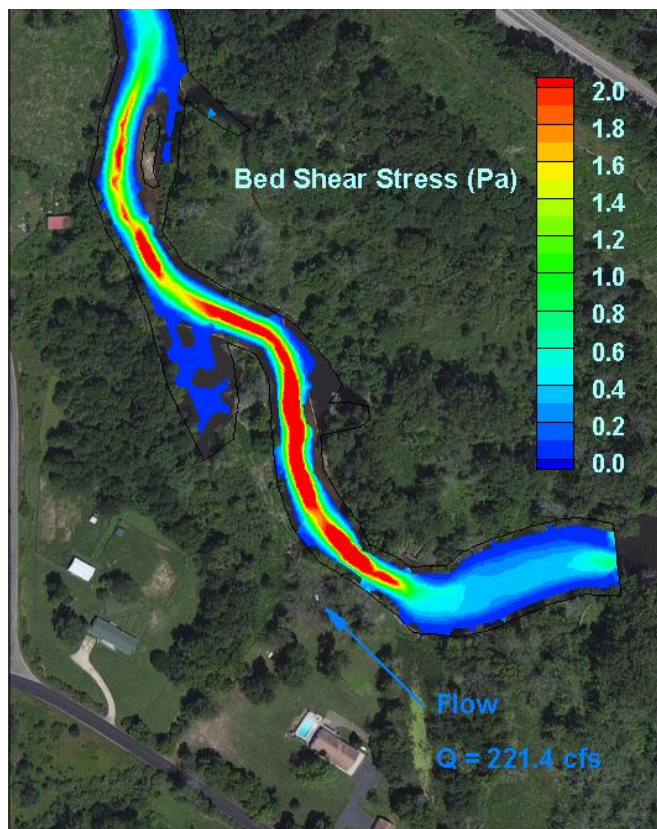


Figure 22. Distribution of Bed Shear Stresses (MP10.4&10.5, 20:00 July 17, 2013)

4. Results of MP 14.75 Sediment Trap Model

4.1 Distribution of Depth-Averaged Velocity Magnitude

Figure 23 and Figure 24 show the depth-averaged velocity magnitude of two flow peaks in the April 2013 high flow scenario. At the first bifurcation, more water flows into the main channel than the side channel; while at the second bifurcation velocity in the north channel is larger than that in the south channel. Figure 25 and Figure 26 show more detailed flow paths at those two bifurcations with a flow discharge of 1332 cfs.

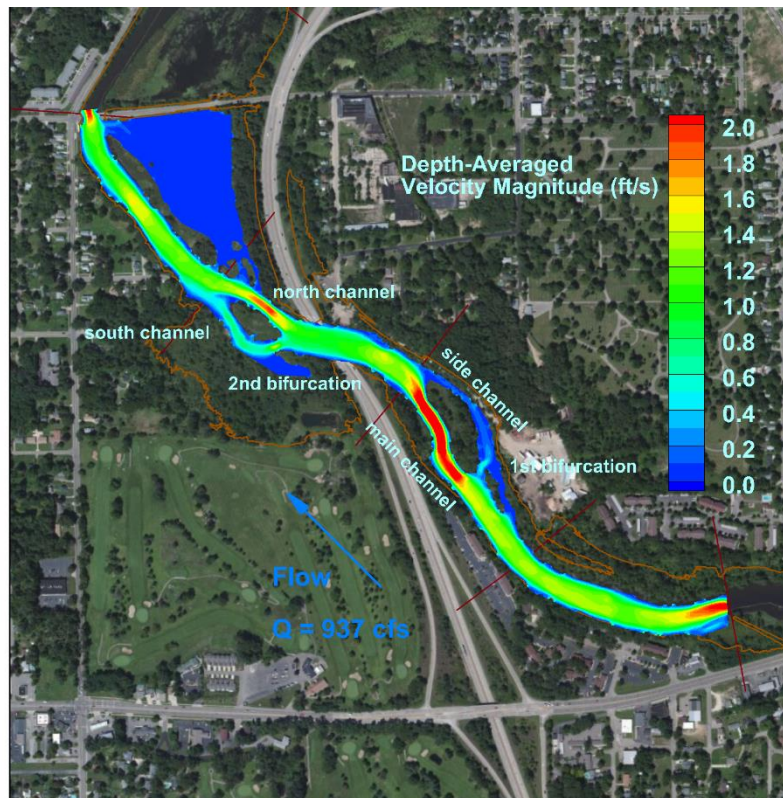


Figure 23. Distribution of Flow Velocity Magnitude (MP14.75, 4:00 April 14, 2013)

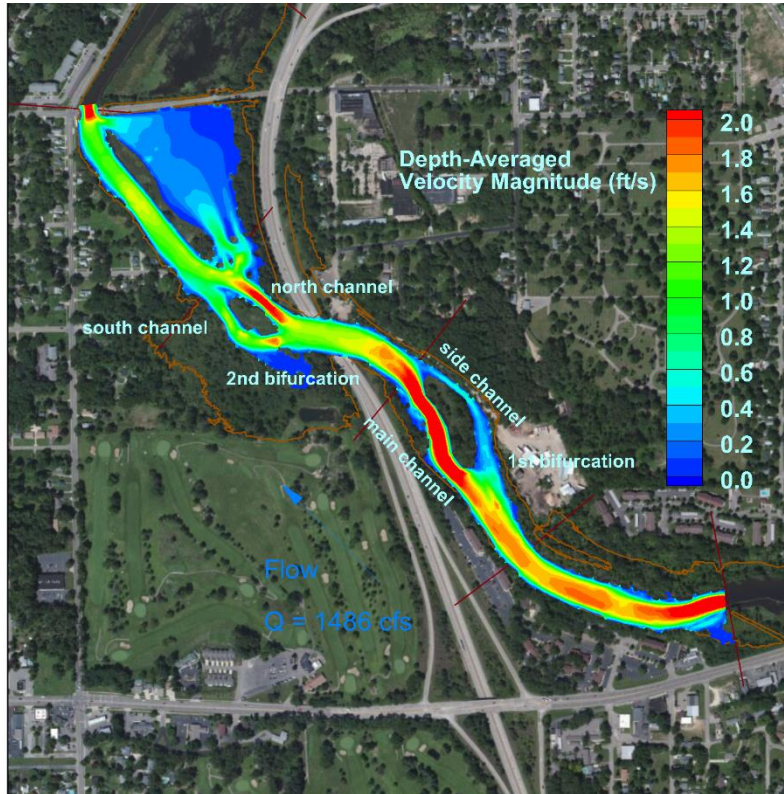


Figure 24. Distribution of Flow Velocity Magnitude (MP14.75, 12:00 April 21, 2013)

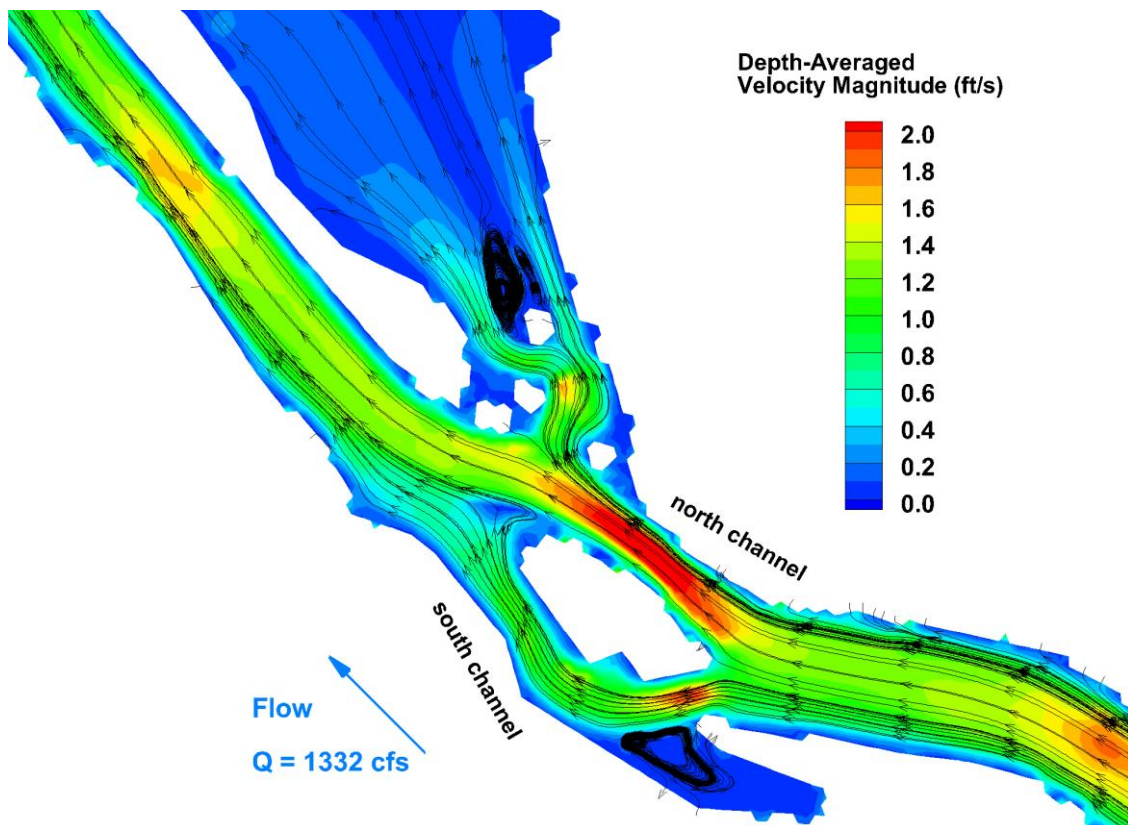


Figure 25. Flow Paths at 2nd Bifurcation and Confluence (MP14.75, 0:00 April 20, 2013)

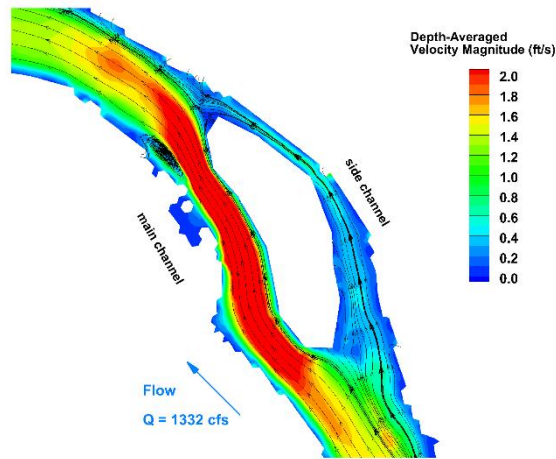


Figure 26. Flow Paths at 1st Bifurcation and Confluence (MP14.75, 0:00 April 20, 2013)

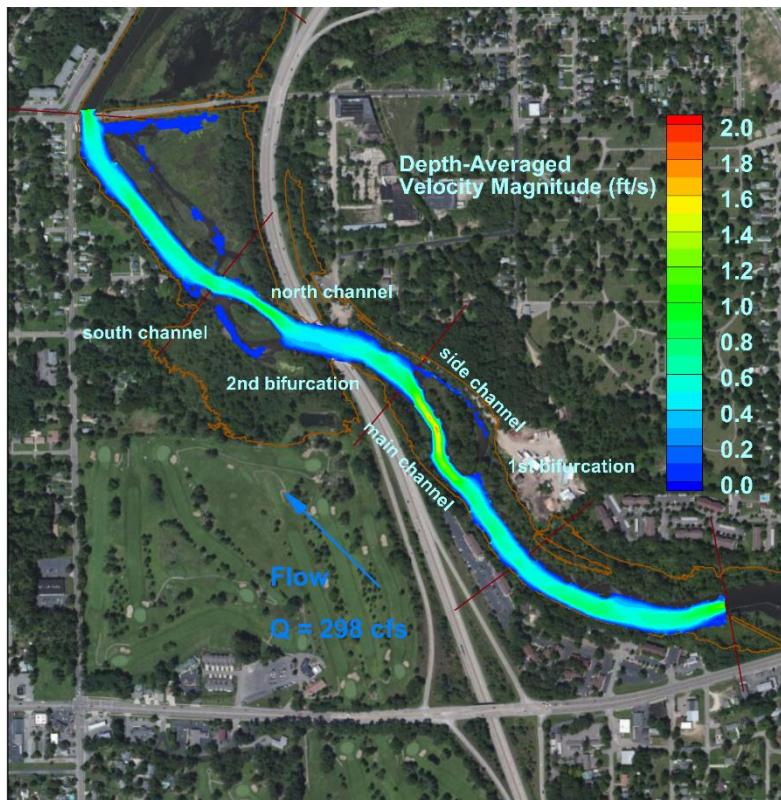


Figure 27. Distribution of Velocity Magnitude (MP14.75, 0:00 July 12, 2013)

Figure 27 shows an example of the velocity distribution in the July 2013 low flow scenario. The discharge was 298 cfs at 0:00 in July 12, 2013. The difference between the velocity magnitude and inundation areas between the two scenarios is evident.

HydroSed2D model is capable of simulating wetting and drying automatically. The

important characteristic of this sediment trap is the channel bifurcation, where the flow separates, and the confluence where the separated flows join again. Sediment deposition and erosion occurs due to the distribution of flow discharge and the change in flow velocities as well as bed shear stresses.

During low flows, the flow follows the main channel only, so that no water and sediment can flow into the bifurcation channel. Also, the sediment load is usually so low that not much morphological change happens. However, high flows can cause significant transport of sediment.

Figure 24 shows that at the first bifurcation more water flows through the main channel than along the side channel. Flow velocities and bed shear stress are much lower in the side channel (see Figure 29). Sediment can be expected to deposit due to reduced flow velocity and associated gradient in bed shear stresses and reduction in sediment transport capacity. At the second bifurcation, more water flows into the north channel, but the south channel flow velocity is not reduced as much as in the first bifurcation. There is a low-velocity zone at the confluence where sediment may deposit. Also, there is a “dead zone” at the south end of the south bifurcation channel which is also a potential depositional area. Immediately after the second confluence, there is another small side channel which bypasses some of the flow into a large floodplain, where deposition can be expected to occur due to much lower velocities.

4.2 Distribution of Bed Shear Stress

Similarly to the above depth-averaged velocity plots, Figure 28, Figure 29, and Figure 30 show distributions of bed shear stress in high and low flow scenarios.

Bed shear stress provides patterns similar to those for velocity magnitude in terms of distribution. Moreover, bed shear stress is a better indicator for sediment transport, especially the fate and transport of oil-particle aggregates (OPAs). In-situ flume and lab experiments suggest that the critical bed shear stress for OPA resuspension may be as low as 0.1 Pa. The areas with less than 0.1 Pa bed shear stresses are most likely areas with large concentrations of submerged oiled sediments.

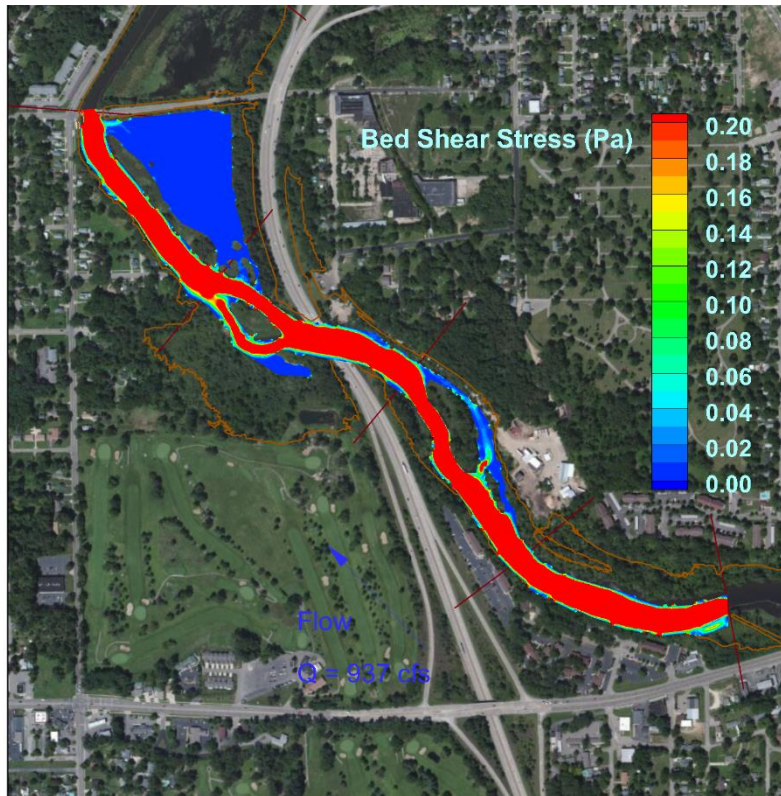


Figure 28. Distribution of Bed Shear Stresses (MP14.75, 4:00 April 14, 2013)

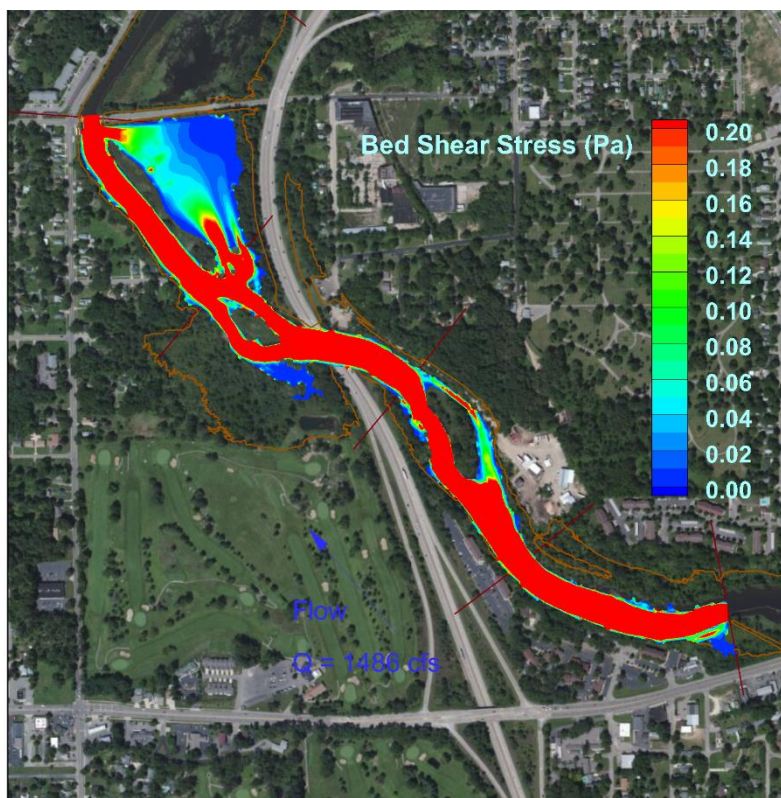


Figure 29. Distribution of Bed Shear Stresses (MP14.75, 12:00 April 21, 2013)

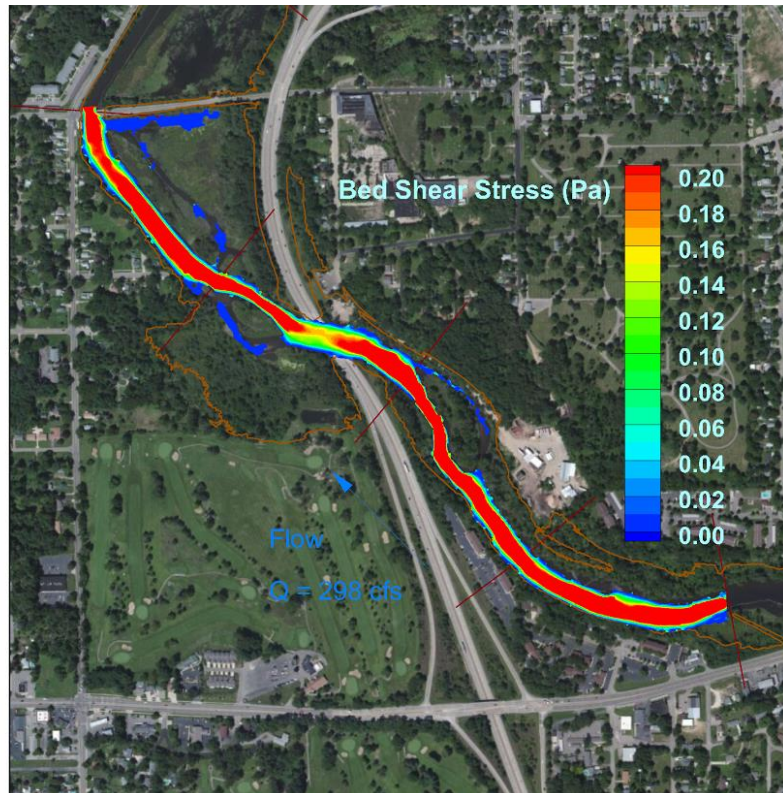


Figure 30. Distribution of Bed Shear Stresses (MP14.75, 0:00 July 12, 2013)

For the high flow scenario during April 20-23, 2013, Figure 29 shows that bed shear stresses for the side channel area are mostly around or higher than 0.1 Pa. A downstream partial barrier was installed here. It seems that such a feature is required for the trap for high flow scenarios. While for the low flow scenario in July 2013, Figure 30 shows that water is flowing only in main channels where bed shear stresses are mostly higher than 0.1 Pa.

4.3 An Example Run: Sediment Transport Simulation (100-year Flood Scenario)

A 100-year flood steady flow scenario was also simulated and used for an example run of sediment transport simulation. This flow scenario was only done for MP14.75 and the sediment transport was only simulated for this flow at MP14.75 sediment trap. The flow discharge is 6,500 cubic feet per second and the downstream water stage level is 830.45 feet. Figure 31 and Figure 32 shows depth-averaged velocity magnitude and bed shear stress, respectively. Moreover, suspended sediment transport is modeled. The inlet

sediment concentration is 130.4 mg/l which was estimated by Dr. David Soong of the USGS (D. Soong, U.S. Geological Survey, written communication 2014). The sediment particle size D_{84} is estimated as 0.2 mm. Figure 33 presents the concentration of suspended sediment. The change of concentration indicates how sediment particles are transported in the domain. The concentration in the sediment trap channel is found to be much lower than that in the main stream before the flow separates. Therefore, the sediment carried by the flow coming into the sediment trap would deposit because of the reduced transport capacity.

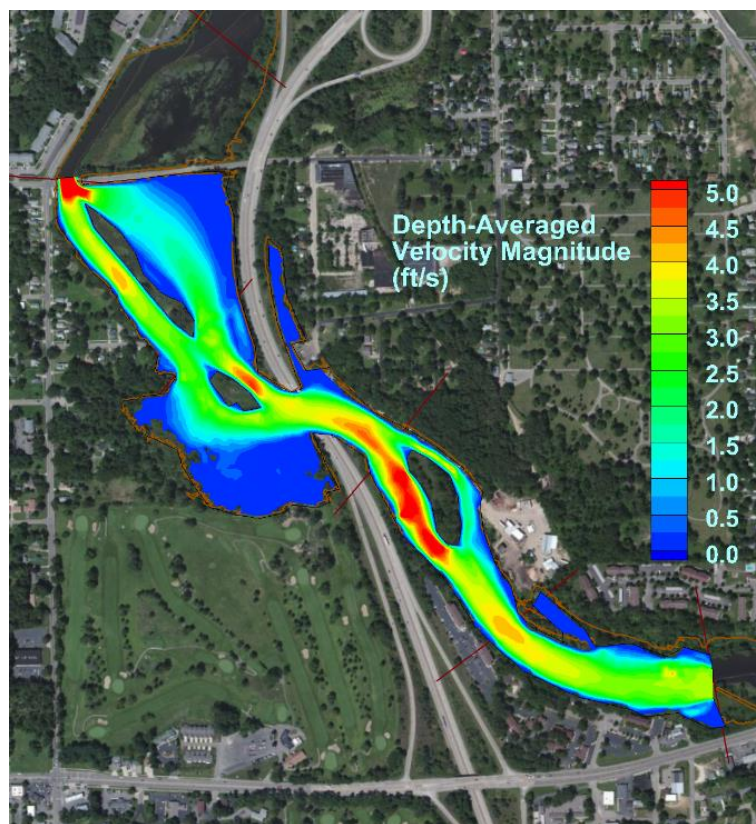


Figure 31. Distribution of Velocity Magnitude in 100-year Flood Scenario (MP14.75)

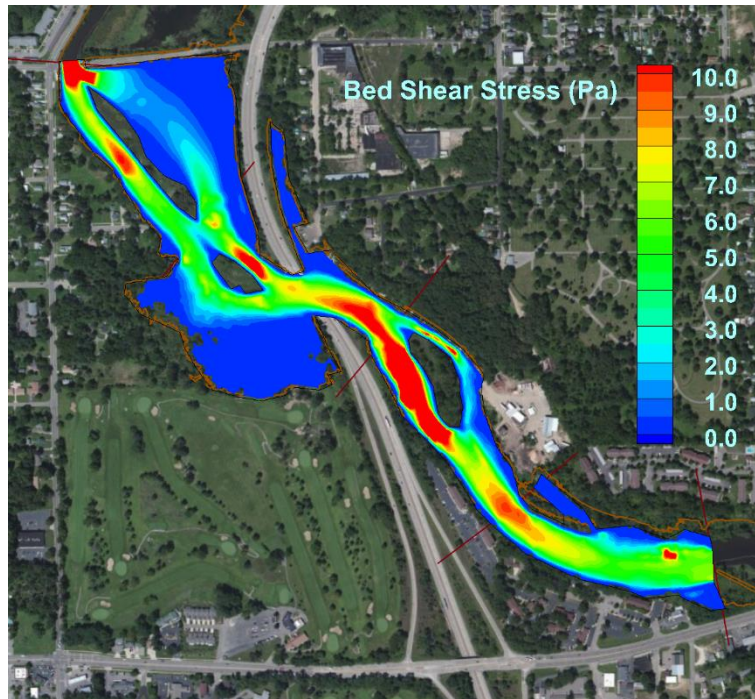


Figure 32. Distribution of Bed Shear Stresses in 100-year Flood Scenario (MP14.75)

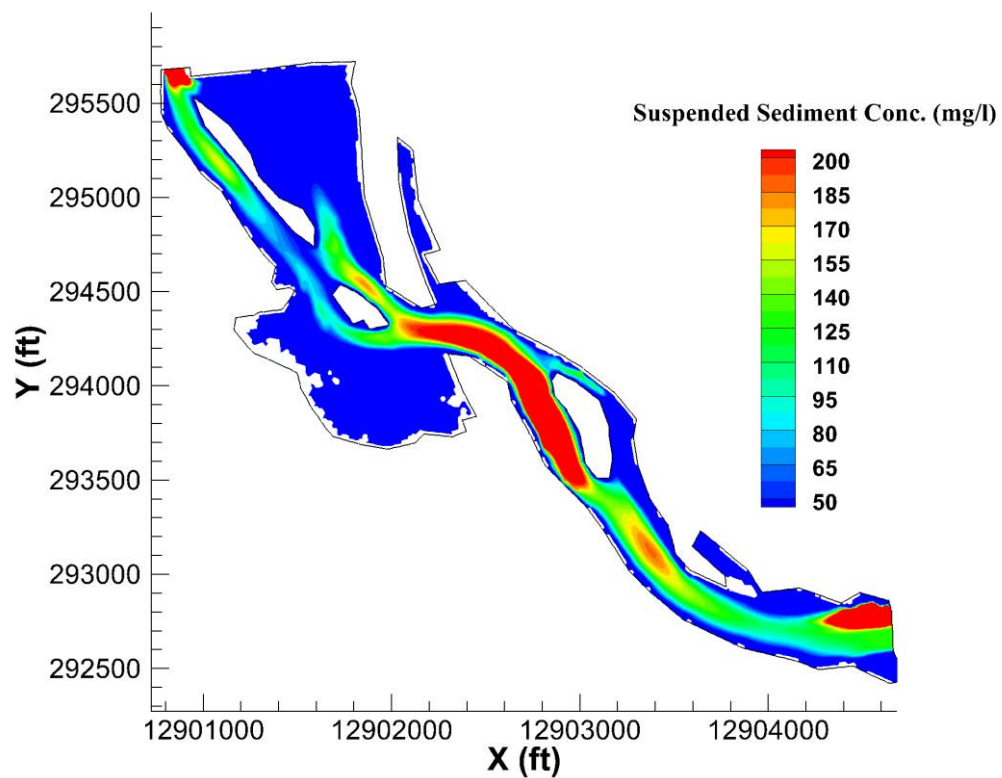


Figure 33. Distribution of Suspended Sediment Concentration in 100-year Flood Scenario (MP14.75)

5. Results of MP 21.5 Sediment Trap Model

5.1 Distribution of Depth-Averaged Velocity Magnitude

Figure 34, Figure 35, and Figure 36 show the depth-averaged velocity magnitude in high flow and low flow scenarios.

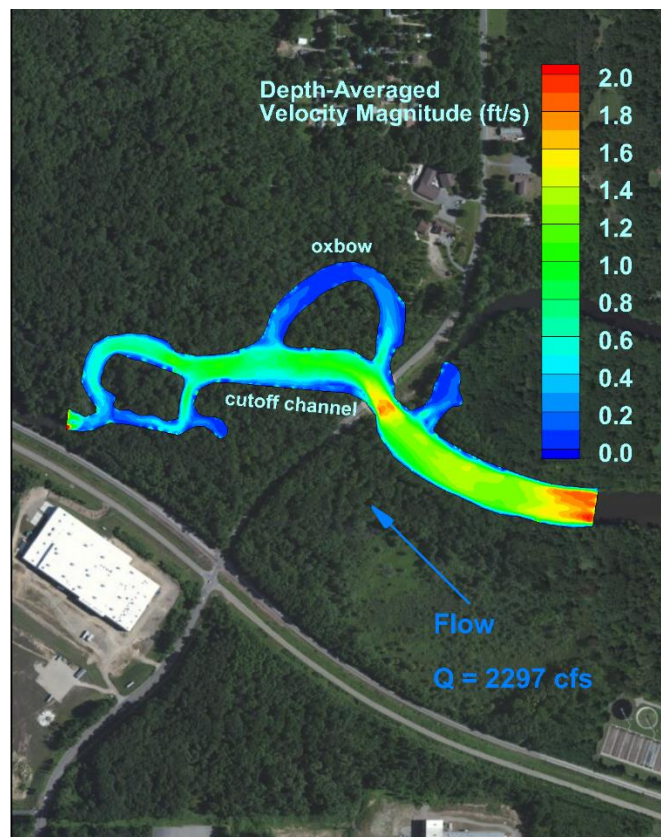


Figure 34. Distribution of Velocity Magnitude (MP21.5, 16:00 April 14, 2013)

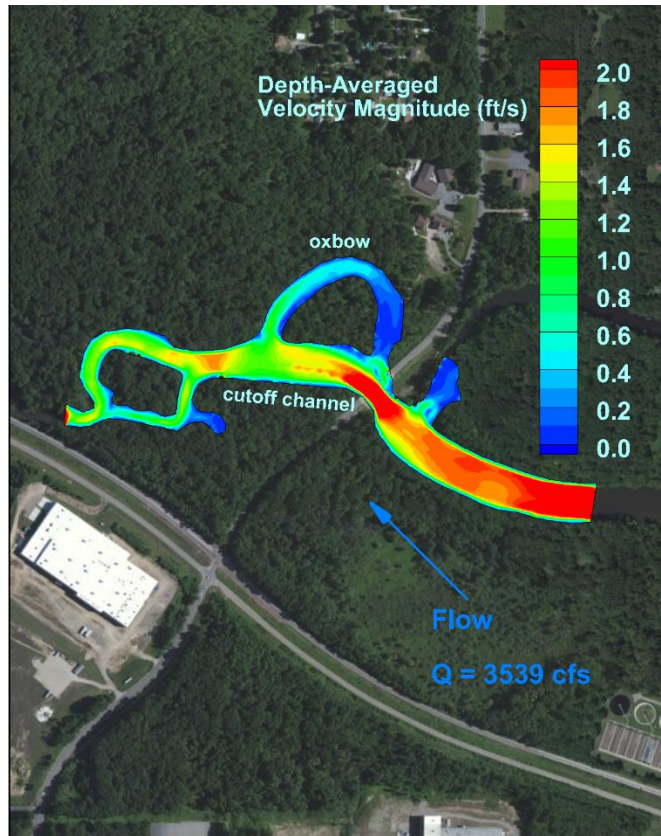


Figure 35. Distribution of Velocity Magnitude (MP21.5, 16:00 April 21, 2013)

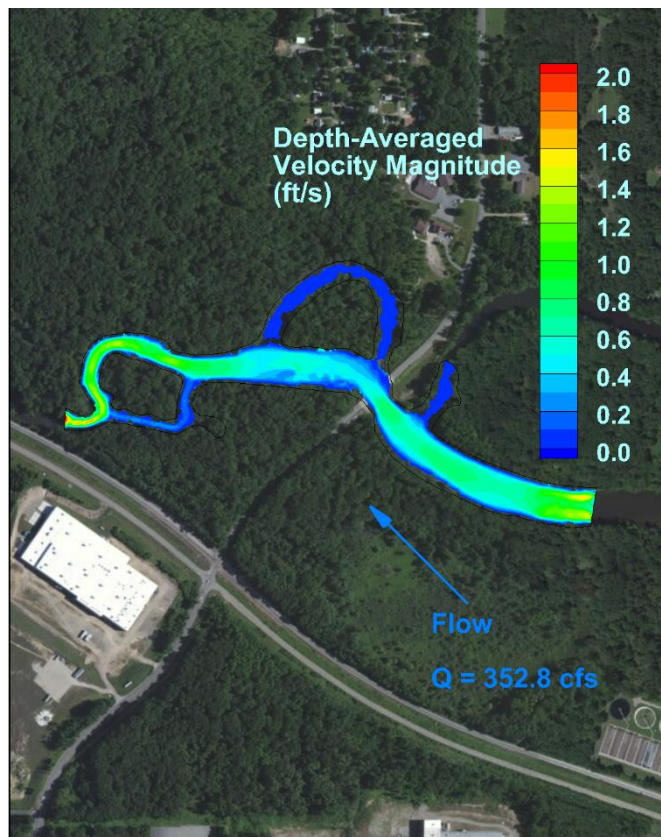


Figure 36. Distribution of Velocity Magnitude (MP21.5, 8:00 July 16, 2013)

The characteristic of this sediment trap is a cutoff channel. During the low flow period, almost no water flows into the original meandering channel. However, during high flows, some water with sediment may flow into the oxbow and sediment or OPAs would deposit therein as Figure 40 indicates.

5.2 Distribution of Bed Shear Stress

Figure 37, Figure 38, and Figure 39 show distributions of bed shear stress under high and low flow scenarios. During high flows, the bed shear stress in main stream is relatively high but once OPAs flow into the oxbow the velocities and bed shear stress become so low that they most likely will deposit. During low flows, even the main stream has low velocities so that OPAs can deposit.

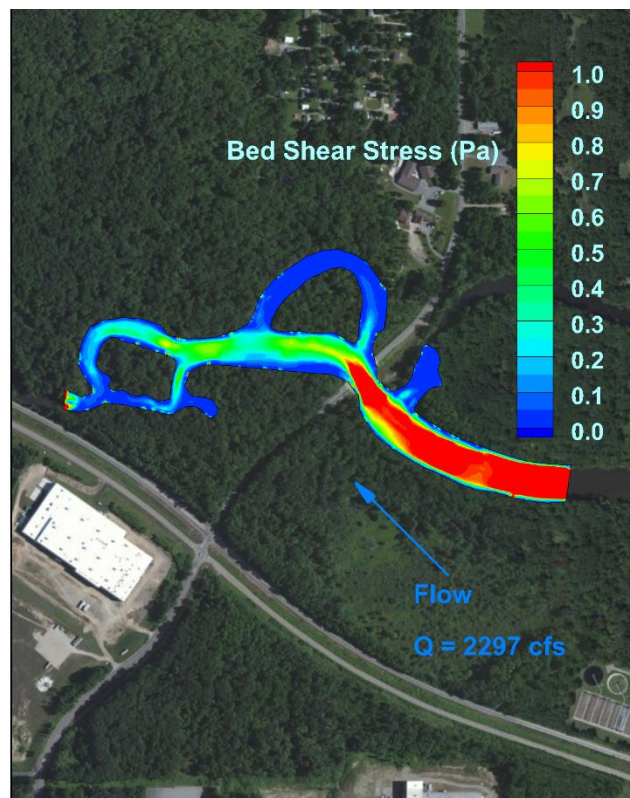


Figure 37. Distribution of Bed Shear Stresses (MP21.5, 16:00 April 14, 2013)

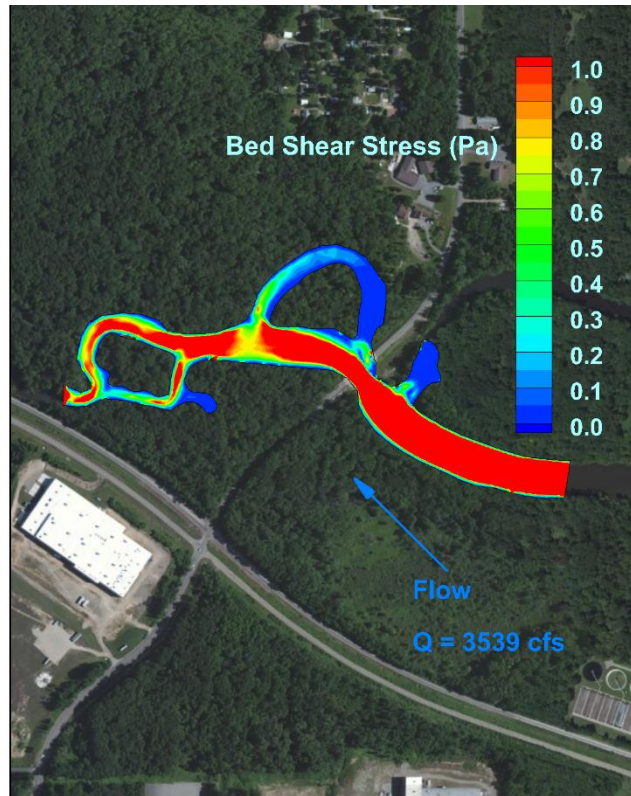


Figure 38. Distribution of Bed Shear Stresses (MP21.5, 16:00 April 21, 2013)

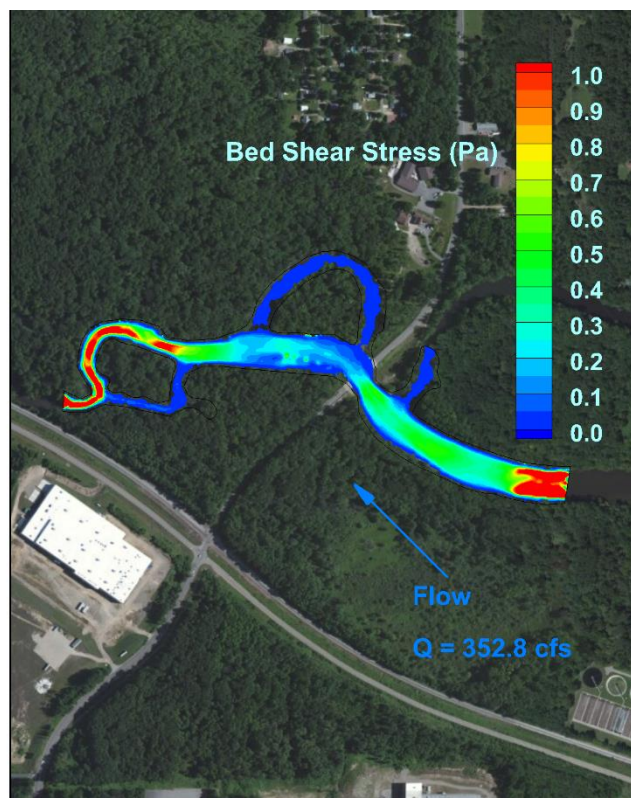


Figure 39. Distribution of Bed Shear Stresses (MP21.5, 8:00 July 16, 2013)

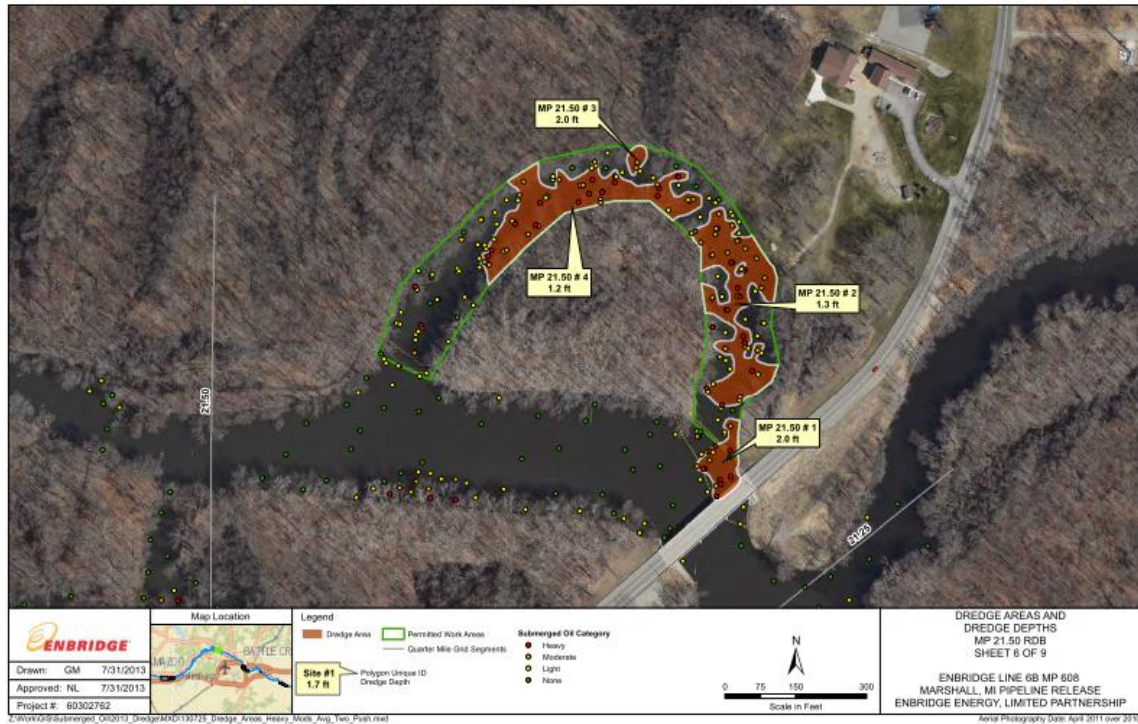


Figure 40. Survey of Submerged Oil in the Modeling Domain of MP 21.5 (figure from the Enbridge Energy, L.P. report [1])

6. Summary

Two-dimensional hydrodynamics models were built for selected sediment traps in Kalamazoo River by applying HydroSed2D. The three natural sediment trap areas have different geometric and morphologic conditions which result in OPAs deposition in the sediment traps. The modeling results were in good agreement with the observed depositional patterns observed in the sediment traps.

The models worked well for different complex topographies and wet-dry conditions. Two flow scenarios were simulated. One was the April 2013 high flow scenario, while the other was the July 2013 low flow scenario. During low flows, no water generally flows into these sediment traps. Deposition happens during relatively high flows when water flows into sediment traps and OPAs would deposit due to gradients in sediment transport capacity associated with low velocities and bed shear stress that were captured by the model predictions.

The depositional areas indicated by the models agree in general with the areas of heavy submerged oil found during the field surveys. The developed models are useful tools in the ongoing cleanup work and may also be useful for future management efforts. For instance, they can be used to evaluate the effects of dredging sediment trapping areas or other engineering efforts for oil removal from the river and its floodplain. It is known that artificial sediment traps were implemented in order to either enhance the trapping efficiency of the natural sediment traps or to create additional trapping areas. The models can be helpful for evaluating the potential impact of such measures as well as in pinpointing what locations might be better suited to capture OPAs.

Acknowledgments

The authors would like to thank Faith Fitzpatrick of the USGS Wisconsin Water Science Center for coordination and help. David Soong of the USGS Illinois Water Science Center is acknowledged for providing advice regarding the modeling and report. Rex Johnson of GRT is acknowledged for providing data and other useful information. Richard D. McCulloch of LimnoTech Inc. is acknowledged for providing the data which was used as boundary conditions of the modeling efforts.

Special thanks are given to U.S. Environmental Protection Agency and Enbridge Energy, L.P., contractors and collaborators involved in assessment and monitoring as well as recovery and containment at the Kalamazoo River site.

Bibliography

1. Enbridge Energy, L.P., Sediment dredge depth and area determination addendum to the 2013 submerged oil removal and assessment work plan (2013).
2. Goodwell, A. E. *et al.* Assessment of floodplain vulnerability during extreme Mississippi river flood 2011. *Environ. Sci. Technol.* **48**, 2619–25 (2014).
3. Liu, X., Landry, B. & Garcia, M. Two-dimensional scour simulations based on coupled model of shallow water equations and sediment transport on unstructured meshes. *Coast. Eng.* **55**, 800–810 (2008).
4. Liu, X. *et al.* Sediment mobility and bed armoring in the St Clair River: insights from hydrodynamic modeling. *Earth Surf. Process. Landforms* **37**, 957–970 (2012).
5. Zhu, Z. Simulation of suspended sediment and contaminant transport in shallow water using two-dimensional depth-averaged model with unstructured meshes. Master Thesis, University of Illinois at Urbana-Champaign (2011).
6. Zhu, Z., Morales, V., Sinha, T. & García, M. Numerical modeling study on the potential impacts of hydraulic structures in the Guayas watershed, Ecuador. *The 7th IAHR Symposium on River, Coastal and Estuarine Morphodynamics (RCEM)* (2011).
7. LimnoTech. Kalamazoo River Hydrodynamic and Sediment Transport Model Documentation (2014).
8. Weston. Bathymetry Report (2014).